

Study the effect of fiber-dia on the alongside dual-plastic optical fiber vibration sensor

Putha Kishore¹ · Dantala Dinakar¹ · Pachava Vengal Rao¹ ·
Kamineni Srimannarayana¹

Received: 21 December 2013 / Accepted: 30 March 2015 / Published online: 19 April 2015
© The Optical Society of India 2015

Abstract An alongside dual-plastic optical fiber vibration sensor is designed based on the reflection intensity modulation and study the effect of transmitting fiber (TF) and receiving fiber (RF) diameter on the sensor response is studied. Three fibers of 0.75, 1 and 1.5 mm diameter are chosen with nine pair combinations for vibration measurement. From displacement response, it is observed that the sensitivity of the sensor increases as the diameter of the RF decreases and vice versa. The test results show that the frequency range increases when the RF diameter is less than the TF and vice versa. The resolution of the sensor also increases when the difference in diameters of the TF and RF decreases and vice versa. Moreover it is evident from the results that the dynamic range, range of frequency can be optimized by choosing the suitable diameter of the TF or RF as for the application.

Keywords Amplitude · Data acquisition · Displacement · Plastic fiber · Vibration sensor · FFT · Frequency

Introduction

Vibration sensors are playing key role in real time monitoring health condition of rotating machinery, where overheating and excessive vibration results in breakdown [1]. Traditional magneto-electric vibration sensors and servo accelerometers have severe shortcomings when used to monitor the vibrations of the engineering structures and machinery. It is well known that

most of the mechanical and electrical vibration sensors need physical contact for these measurement. On the other hand some of the optical sensors need not require any physical attachment with sensing area and does not perturb the source of vibration [2]. According to the working principle of the optical fiber vibration sensors which are divided into two types; i) phase modulation and ii) intensity modulation. First one uses interference such as Michelson or Mach-Zehnder interferometer [3], self-mixing [4] and Doppler vibrometry [5, 6] to interrogate the phase shift caused by vibration. These methods exhibit high sensitivity and excellent performance but suffer from low stability and stringent mechanical requirements. Because of its complex and expensive setups limit their practical use and not well suited to map the amplitude of vibration in several test points [7]. Second one takes the advantage of change in intensity corresponding to vibration using PMMA fiber optic sensor [8, 9]. Presence of advantages like low-cost, stable and portable sensor for the detection of vibration has led to this work to study the effect of diameter of the transmitting and receiving fibers on sensing.

In this paper, designed a dual plastic optical fiber vibration sensor is designed and demonstrated to study the performance of the sensor for different combinations of the TF and RF. The sensor design consists of six fibers with three diameters, forming nine pair combinations, a LED light source, a photo-detector with transimpedance amplifier to convert light intensity into equivalent voltage signal and a Data Acquisition system used for record and monitoring of the vibration.

The sensor working principle

The sensor head is placed in such a way that the axis of the fiber optic pair is perpendicular to the targeted area of the vibration sensing. Vibration measurement has been made using different combinations fiber optic pairs with respect to

✉ Putha Kishore
Kishorephd.nitw@gmail.com

¹ Department of Physics, National Institute of Technology Warangal, Warangal, India

diameter. The light from the source is coupled to one end of the TF then passes through it and falls on the vibrating target. The light reflected from the reflecting surface of the vibrating target is coupled to one end of the RF.

According to the light intensity distribution function, the irradiance of emitted light from TF is expressed as

$$I(r, z) = \frac{2P(z)}{\pi\omega^2} \exp\left[\frac{-2r^2}{\omega^2(z)}\right] \quad (1)$$

Where r and z is the radial and longitudinal coordinates respectively, $\omega(z)$ is the beam radius which is also the function of z and is expressed as

$$\omega(z) = \omega_o \sqrt{1 + \left(\frac{z}{z_R}\right)^2} \quad (2)$$

$$Z_R = \sqrt{\frac{\pi\omega_o^2}{\lambda}} \quad (3)$$

Where ω_o the beam waist radius and Z_R the Rayleigh range, these are important parameters of the beam distribution function. The amount of reflected light received by the RF from the target is evaluated by integrating the irradiance over the core area of S_r

$$P(z) = \int_{sr}^0 I(r, z) ds_r, \quad (4)$$

Thus the amount of reflected light collected by the RF is a function of the displacement between probe and target (reflecting surface) can be expressed as [10, 11]

$$P(z) = \frac{2P_E}{\pi\omega^2(z)} \int_{y=-R_r}^{R_r} \int_{x=m_1}^{m_2} \exp\left[\frac{-2(x^2 + y^2)}{\omega^2(z)}\right] dx dy \quad (5)$$

Where $m_1 = R_t + R_r + R_d - \sqrt{R_r^2 - y^2}$ and $m_2 = R_t + R_r + R_d + \sqrt{R_r^2 - y^2}$, P_E is the power of light from

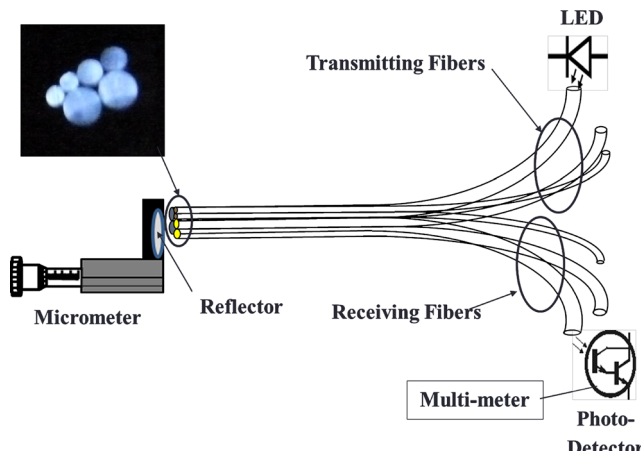


Fig. 1 The schematic of experimental set up used for the calibration

Table 1 Parameters of the PMMA optical fibers

S. No.	Optical fiber outer diameter (mm)	Core diameter (mm)	Cladding diameter (mm)	Numerical aperture (NA)
1	1.5	1.470	1.5	0.5
2	1.00	0.98	1.00	0.5
3	0.75	0.735	0.75	0.5

the TF incident on the reflector, R_t and R_r are the core radius of TF and RF respectively and R_d is the distance between the center of RF and TF cores.

A simple photo-detection circuit is used to convert the light intensity into equivalent voltage. Generally, the output voltage with respect to the intensity of light incident on photo-detector is given by [12]

$$V_{out} = R_\lambda P R_E \quad (6)$$

Where $R_\lambda = \eta g \frac{\lambda}{1.24}$ is the responsivity of the photo-detector, R_E is the feedback resistance, η , λ and g are the quantum efficiency, wavelength of the incident light and photoconductive gain respectively. For a given photo detector the values of (<1) and g are the constants, therefore the responsivity (sensitivity) is dependent only on the wavelength of the light. Thus the selection of source and detector should be matched.

Experimental setup

Before measuring the vibration sensor has been calibrated by studying the displacement response, from which the linear region is considered suitable for vibration measurement. The schematic experimental setup for the fiber optic displacement response is shown in Fig. 1. It consists of a light source, a flat mirror, a photo detector along with required electronic circuit. The sensor head contains a bundle of plastic fibers made up of

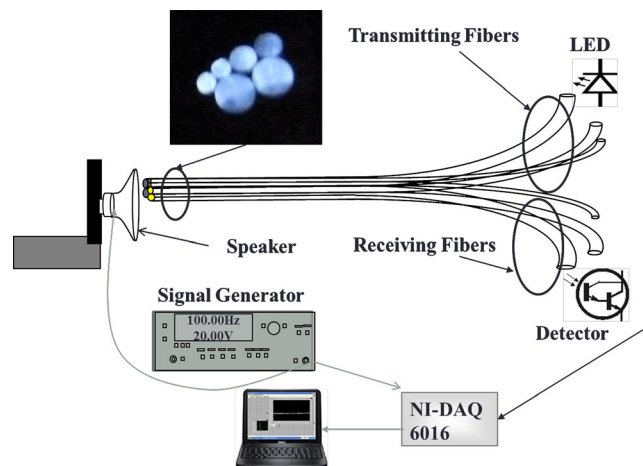


Fig. 2 Schematic experimental setup for vibration measurement

Table 2 Comparison of displacement response for all the combinations

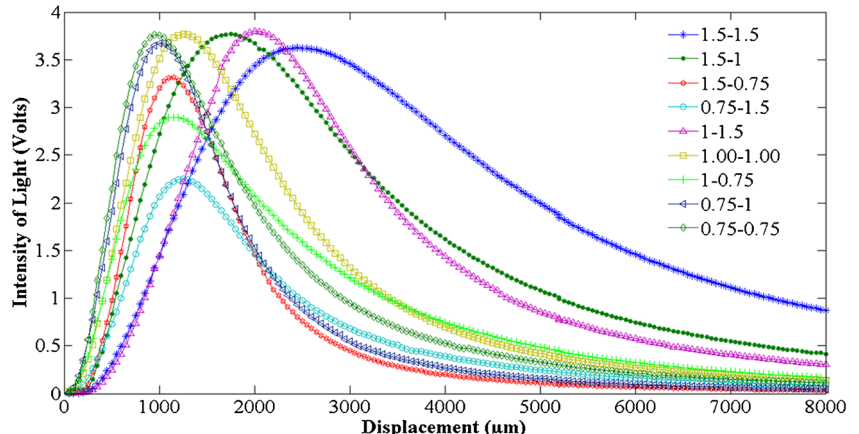
S. No.	Combination (mm)	Linearity range of front slope (μm)	Sensitivity of front slope (mv/ μm)	Linearity range of back slope (μm)	Sensitivity of back slope (mv/ μm)
1	1.5–1.5	850(700–1550)	2.435	1300(4400–3100)	0.763
2	1.5–1.00	650(500–1150)	3.544	900(3500–2600)	1.124
3	1.5–0.75	500(400–900)	4.838	600(2000–1400)	2.531
4	1.00–1.00	450(350–800)	4.786	1000(1600–2600)	1.696
5	1.00–1.5	700(300–1000)	2.574	1000(1450–2450)	1.134
6	1.00–0.75	450(300–750)	3.9488	800(2100–2900)	0.855
7	0.75–0.75	400(250–650)	6.1975	700(1150–1850)	1.98
8	0.75–1.5	550(400–950)	2.727	800(1400–2200)	1.181
9	0.75–1.00	350(300–650)	5.694	450(1350–1800)	2.74

Polymethyl methacrylate (PMMA) of length 50 cm, configured with six fibers having three different diameters forming nine combinational pairs. That is, there are three transmitting fibers of 0.75, 1, and 1.5 mm diameter, and three receiving fibers corresponding to those same diameters with possible pair combinations. Thin plastic reflector is used as a reflecting surface which is glued to the translation stage for the calibration. A LED (IF-E96) is used as light source having typical peak wavelength at 650 nm which is one of the optical transmission windows of the PMMA fiber. One end of the RF is fixed to highly sensitive photo Darlington transistor (IF-D93) used as a photo-detector which is matched to the visible region.

The experiments are carried out for three different fiber diameters forming 9 pair combinations (both TF and RF). Optical fiber (i-fiberoptics, Super Eska) parameters which are used in this investigation are tabulated in Table 1. In this investigation, the effect of diameter of the fiber on the vibration sensing is studied, so that the fibers which are taken have same numerical aperture. It is well known that the NA of the fiber represents the acceptance of the light and it depends only the refractive indices of core and clad of the optical fiber but not on the diameter of the fiber [13]. Thus the response of the sensor depends only on geometrical parameters of the optical

fiber and design configuration. The sensing window of the plastic fiber is in the region of visible light between 500 and 700 nm. However, from the attenuation loss of the PMMA step index fiber nearly 520, 570 and 650 nm showing low attenuation and are suitable sources for transmission and sensing application [14, 15]. The photo-detector (IFD-93) also has the high responsivity at 650 nm is used for sensing the intensity of light from the output of the optical fiber. The cost of this source is very cheap when compared to other light sources. The front view of the sensor probe is shown in Fig. 1. The LED light is coupled to one end of the TF and is directed to incident on the mirror. The reflected light from the reflecting surface is received by the RF of the sensor probe and routed to incident on the photo-detector. The photon energy collected by the detector is converted into its equivalent voltage using simple detection circuit and is connected to digital multi meter to record or monitor the voltage signal. The distance between the fiber probe and the mirror is moved in steps of 50 μm and measured the corresponding output voltage, which represents the optical power. The same experiment is repeated for different pair combinations.

The schematic experimental setup for vibration measurement is shown in Fig. 2. It consists some additional

Fig. 3 Displacement response for all the combinations

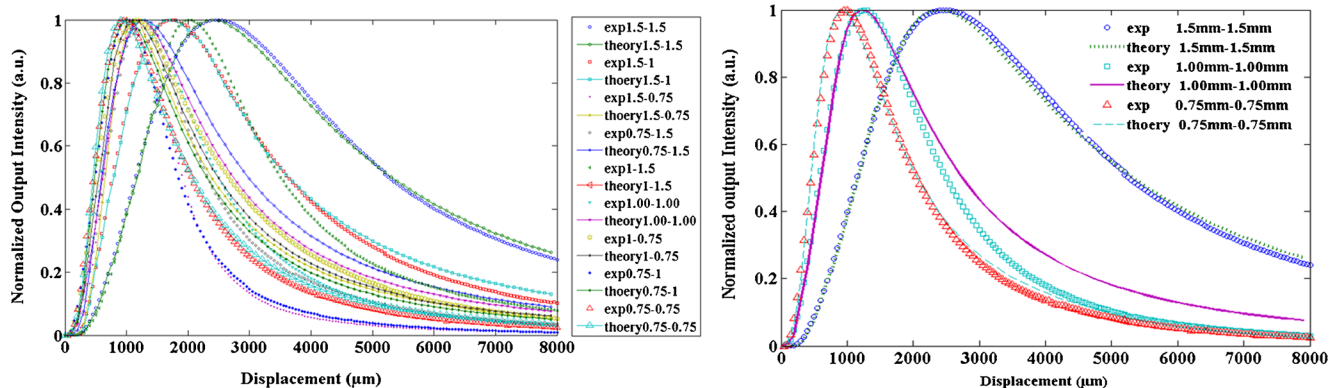


Fig. 4 Comparison between experimental and theoretical results of displacement response corresponds to all the combinations

equipment's; data acquisition (DAQ), computer, speaker, function generator, power amplifier and calibrated mirror. The calibrated reflector is glued to the center of the speaker diaphragm which is replaced the translation stage. A portable high performance multifunction data acquisition system from National Instruments (NI-DAQpad-6016), and LabVIEW software is used for continuous monitoring of vibrations. DAQ has 16 bit resolution, maximum sampling rate of 200 KS/s and maximum input signal range of ± 10 V. The time domain data signal is converted into frequency domain signal using FFT (fast Fourier transform) technique.

Results and discussions

Displacement response of the sensor

The displacement response of the sensor exhibits two linear regions namely front slope and back slope. The detector output shows minimal at zero distance between reflecting target and sensor probe because the reflecting light cone of the TF does not reach the receiving cone of RF. As the distance from the sensor probe increases the cone size of the transmitted light on

the reflecting surface also increases which starts to overlap with the RF cone area leading to a small output voltage. Further increase in distance between sensor probe and reflector leads to larger overlapping results in increase in the intensity of light at other end of the RF fiber. The intensity of light is converted into equivalent voltage using transimpedance amplifier circuit. However after reaching the maximum value at certain distance indicates that the complete overlapping of the RF with TF reflecting cone, afterwards the output voltage starts decreasing even though the distance increased. Because the large increase in the size of the reflecting light cone leading to decrease in power density but the area of overlapping remains constant. The experiment is repeated with different combination of TR-RF diameters as given in Table 2 and the displacement response for all these combinations are plotted in Fig. 3. Figure 4 shows the normalized intensity plot to compare the experimental and simulation (using Eq. (5)) results. It is The front slope of the all the combinations is exactly matched whereas back slope exhibits a bit of mismatch with theoretical results, it may be occurred due to domination of the stray light interference and parameter values used for simulation may not be exactly matched with real values. Therefore front slope is used to measure the vibration.

The sensitivity and linearity of both front and back slopes of all the combinations are summarized in Table 2. The pair

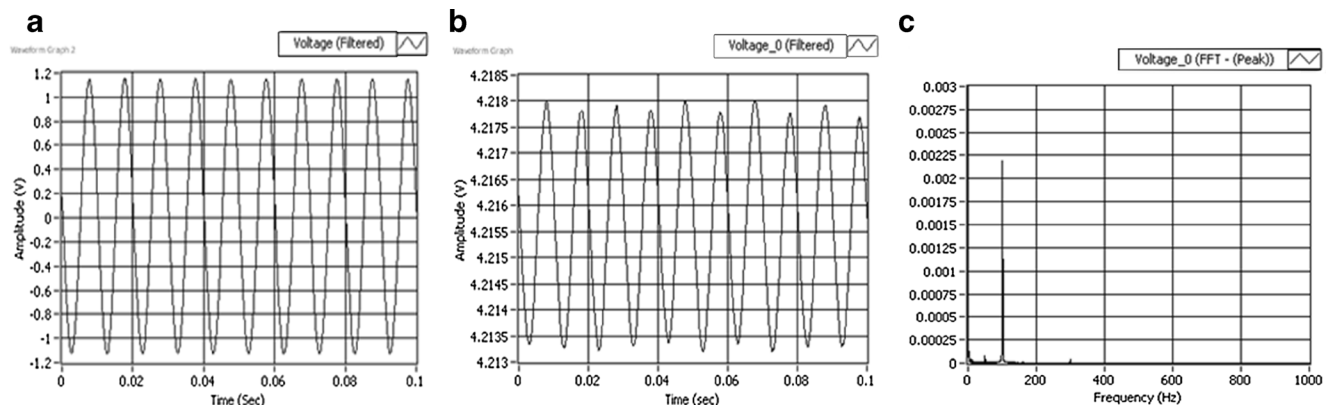


Fig. 5 **a** sensing signal, **b** reference signal and **c** FFT (frequency spectrum) of the sensing signal

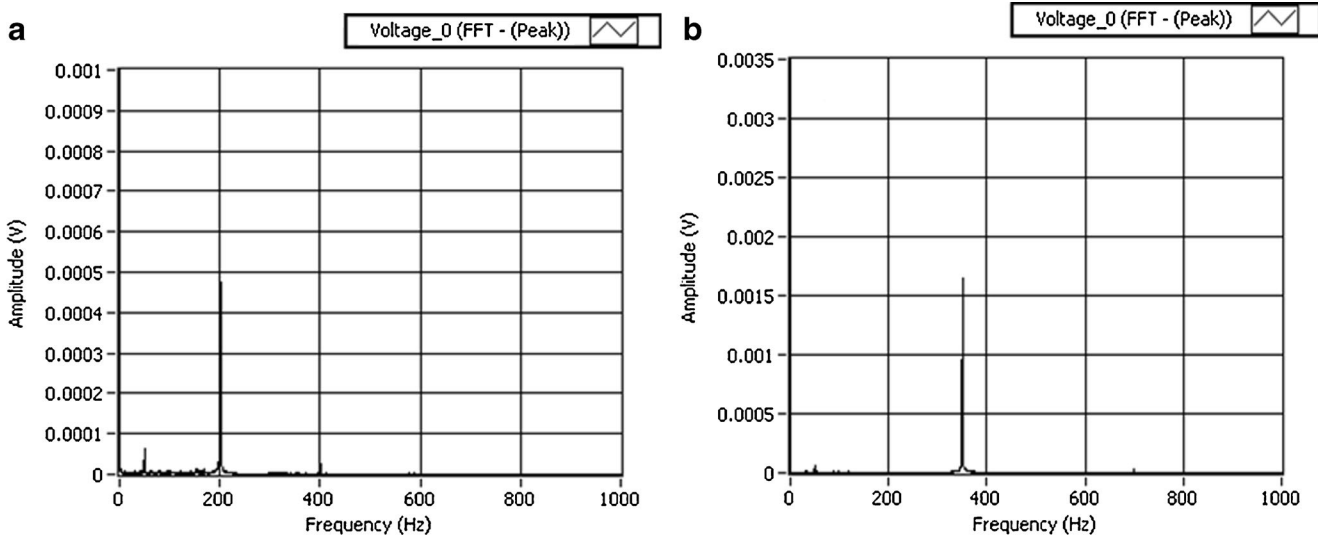


Fig. 6 The frequency spectrum of the sensing signal at different frequencies **(a)** 200Hz and **(b)** 350Hz

combination 1.5–1.5 mm shows the large linear range of 850 and 1300 μm for both the front and back slopes respectively. Because it has the largest receiving fiber diameter able to collect more reflected light. But it exhibits low sensitivity. The highest sensitivity for front and back slopes obtained are 6.1975 and 1.98 mV/ μm respectively for the combination of 0.75–0.75 mm. It is observed from the results that as the diameter of one of the optical fiber or both fibers in pair decreases sensitivity of the sensor increases which means that the sharp change in intensity for very small variation of the displacement (amplitude) results in high resolution.

Measurement of vibration

To determine the vibration, the sensor probe is mounted normally to the reflector which is glued at the center of the

speaker. The initial position of the fiber probe from reflector is determined from the displacement response curve of the sensor as shown in Fig. 3. The front slope is used for extremely small amplitude of vibration measurement and for high sensitivity.

For the fiber pair combination 1.5–1.5 mm, the front slope having sensitivity of 2.435 mV/ μm is used for the vibration measurement and the sensor probe is placed such that the detector output situated within the linear region of the slope of about 850 μm (700–1550 μm). The output voltage from photo-detector is connected to the DAQ pad and the data are recorded by the LabVIEW and saved for future analysis. The time domain signal (TDS) gives the real time monitoring of the vibration. The frequency response of the sensor is observed by recording the sensing signal and processed by FFT technique. The vibration measurement signal of the sensor is shown in Fig. 5 at a frequency of 100Hz, Fig. 5a Shows

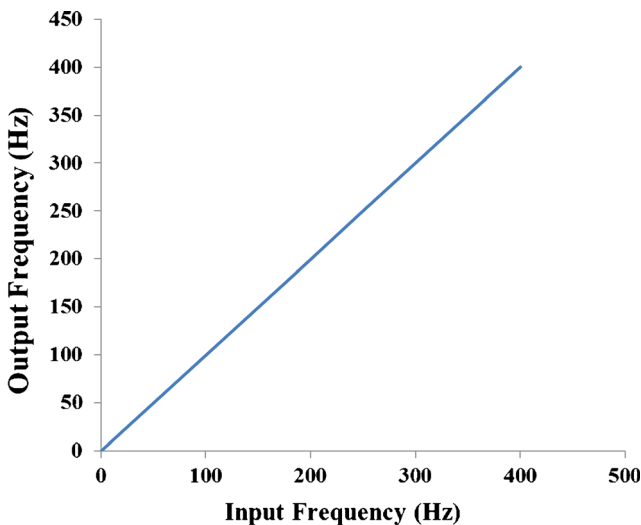


Fig. 7 The frequency response of the sensor for 1.5–1.5 mm combination

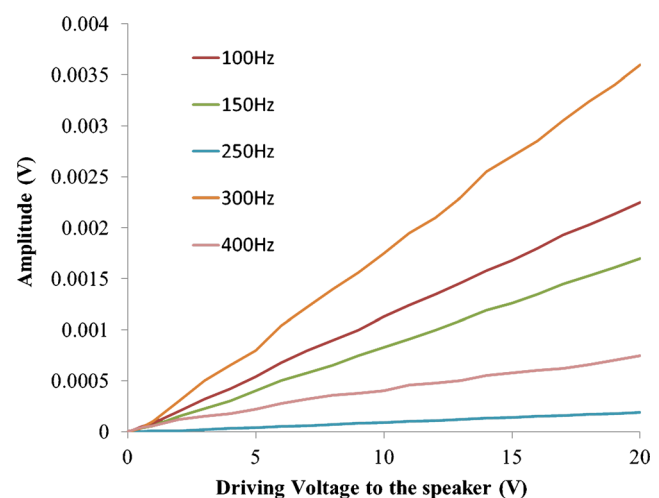


Fig. 8 Amplitude response of the sensor for 1.5–1.5 mm combination at different frequencies

Table 3 Comparison of sensor response corresponding to vibration for different pair combinations

S.no	Combination (mm)	Resolution (mv)	Frequency range(Hz)	Resolution(μm)
1	1.5–1.5	0.000005	0–400	2.053388
2	1.5–1.00	0.000003	0–600	0.8465
3	1.5–0.75	0.000002	0–700	0.4133
4	1.00–1.5	0.000009	0–800	3.49650
5	1.00–1.00	0.000002	0–900	0.4178
6	1.00–0.75	0.000001	0–950	0.253241
7	0.75–1.5	0.0000016	0–1050	0.586725
8	0.75–1.00	0.0000021	0–1100	0.368809
9	0.75–0.75	0.000001	0–1200	0.16135

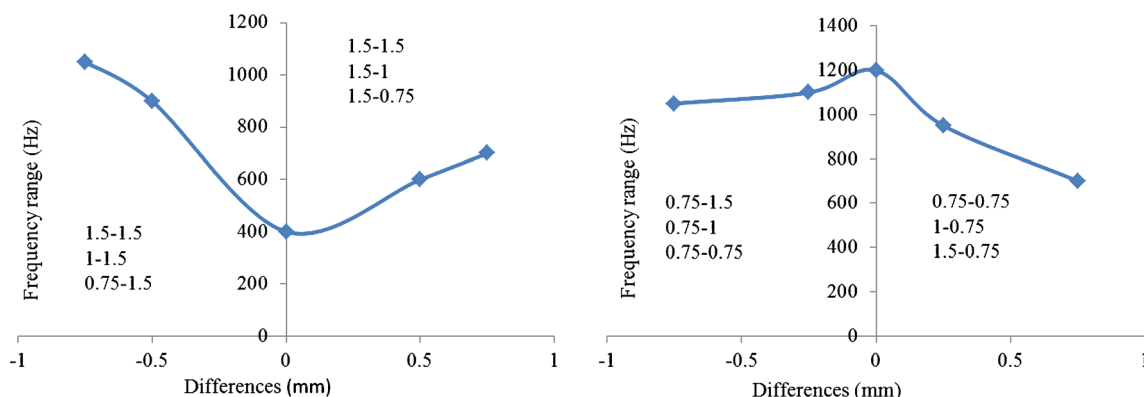


Fig. 9 Frequency range variation with combination of **a** 1.5 mm and **b** 0.75 mm

Fig. 10 Frequency range variation with combination of 1 mm as **a** transmitting fiber and **b** receiving fiber

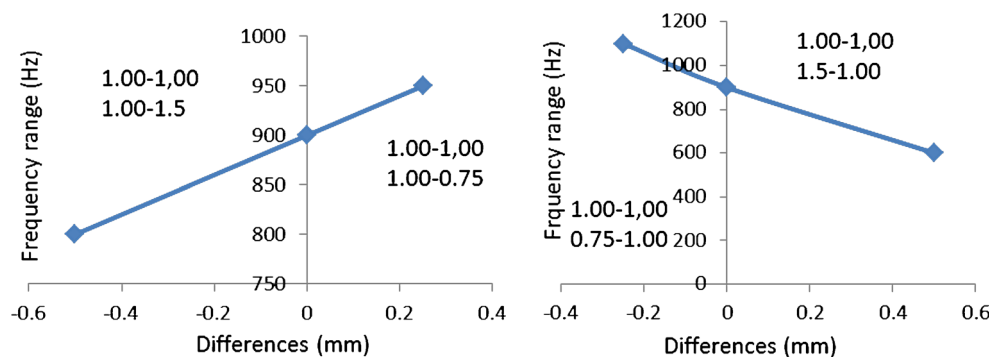


Fig. 11 Resolution variation with combination of **a** 1.5 mm and **b** 0.75 mm

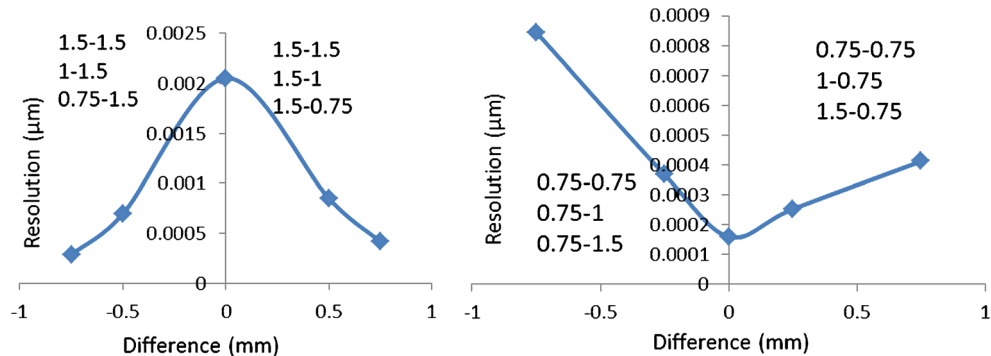
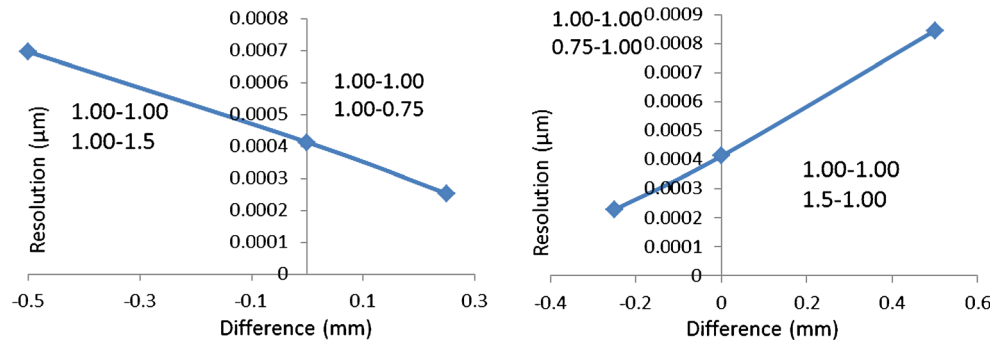


Fig. 12 Resolution variation with combination of 1 mm as **a** transmitting fiber and **b** receiving fiber



the TDS signal of the sensing signal measured by the sensor, Fig. 5b shows the TDS of the reference signal given to the speaker using signal generator and Fig. 5c shows the (FFT) frequency spectrum of the sensing signal. The FFT spectrum measured by the sensor for the vibration at different frequencies are shown in Fig. 6.

The frequency response of the sensor is shown in Fig. 7, and it is observed that there is good matching between input frequency applied to the speaker and frequency sensed by the sensor up to 400Hz, above 400Hz an error of $\pm 5\%$ is observed. The amplitude response of the sensor is plotted by varying the driving voltage (0–20 V) to the speaker at different frequencies, as shown in Fig. 8. To test the reliability of the sensor, the experiment is repeated several times and found that the sensor response is consistent with small error of 2 %.

The same experiment is repeated for other combinations which are tabulated in Table 2. The obtained results from sensor vibration response corresponding to different fiber pair combinations are tabulated in Table 3. Figure 9a represents the frequency range variation in the pair combination 1.5 mm as one of the fibers, as the modulus of difference between RF and TF increases the frequency range also increases. That is among the two fibers of sensor pair one fiber always 1.5 mm, In the right side of the graph TF is constant of 1.5 mm and the RF diameter is decreased. On the left side of the graph RF diameter is constant and TF diameter is decreased. Figure 9b represents the frequency range variation in the pair combination 0.75 mm as one of the fibers, as the modulus of difference between RF and TF increases the frequency range is decreases. Figure 10a shows that as the difference between TF (1 mm) and RF increases the range of frequency also increases whereas in Fig. 10b the difference between the TF and RF (1 mm) increases the frequency range is decreased. From the above results it is illustrated that the smaller the diameter of either TF or RF shows large frequency range and also it has been observed that smaller the diameter of TF than RF shows large range of frequency.

Figure 11a represents the resolution variation in the pair combination 1.5 mm as one of the fibers, as the modulus of difference between RF and TF increase the resolution also improved. Figure 11b represents the frequency range variation

in the pair combination 0.75 mm as one of the fibers, as the modulus of difference between RF and TF increase the resolution becoming low. Figure 12 shows that the difference between the TF (1 mm) and RF increases the resolution also improved whereas difference between the TF and RF (1 mm) increases the resolution falling down. From the above results it is illustrate that the smaller the diameter of either TF or RF shows high resolution, however it can be observed that smaller the fiber diameter of TF than RF shows high resolution.

Conclusions

The plastic optical fiber vibration sensor is designed and demonstrated using different fiber pair combinations. From displacement response, it is evident that the sensitivity of the sensor increases as the diameter of the fiber decreases and vice versa. The vibration measurements of all the combinations show that the frequency range and resolution are increased when the fiber diameter decreases. Moreover it is evident from the results that the dynamic range, range of frequency can be optimized by the suitable diameter of the fiber.

References

1. J.D. Zook, W.R. Herb, C.J. Bassett, T. Stark, J.N. Schoess, M.L. Wilson, Fiber-optic vibration sensor based on frequency modulation of light-excited oscillators. *Sensors Actuators* **83**, 270–276 (2000)
2. A. Buffa, G. Perrone, A. Vallan, A plastic optical fiber sensor for vibration measurements, *I2MTC 2008 - IEEE international instrumentation and measurement technology conference Victoria, Vancouver Island, Canada, 12–15 May 2008*
3. S. Donati, *Electro-optical instrumentation: sensing and measuring with lasers* (Prentice Hall, Upper Saddle River, 2004)
4. G. Giuliani, M. Norgia, S. Donati, T. Bosch, Laser diode self-mixin technique for sensing applications. *J. Opt. A Pure Appl. Opt.* **4**, S283–S294 (2002)
5. P. Castellini, M. Martarelli, E.P. Tomasini, Laser Doppler vibrometry: development of advanced solutions answering to

technology's needs. *Mech. Syst. Signal Process.* **20**, 1265–1285 (2006)

- 6. A. Chijioke, J. Lawall, Laser Doppler vibrometer employing active frequency feedback. *Appl. Opt.* **47**, 4952–4958 (2008)
- 7. J. Chang, Q. Wang, X. Zhang, D. Huo, L. Ma, X. Liu, T. Liu, C. Wang, A fiber Bragg grating acceleration sensor interrogated by a DFB laser diode. *Laser Phys.* **19**(1), 134–137 (2009)
- 8. S. Binu, K. Kochunaranayanan, V.P. Mahadevan Pillai, N. Chandrasekaran, PMMA (Polymethyl Methacrylate) fiber optic probe as a noncontact liquid level sensor. *Microw. Opt. Technol. Lett.* **52**(9), 2114–2118 (2010)
- 9. P. Kishore et al., Fiber optic vibration sensor using PMMA fiber for real time monitoring. *Sens. Transducers* **136**(1), 50–58 (2012)
- 10. S. Wadi Harun, H.Z. Yang, M. Yasin, H. Ahmad, Theoretical and experimental study on the fiber optic displacement sensor with two receiving fibers. *Microw. Opt. Technol. Lett.* **52**(2), 373–375 (2010)
- 11. P.B. Buchade, A.D. Shaligram, Influence of fiber geometry on the performance of two-fiber displacement sensor. *Sensors Actuators A* **136**, 199–20 (2007)
- 12. E. Rosencher, B. Vinter, *Optoelectronics, English edition* (Cambridge University Press, Cambridge, 2004), pp. 475–509
- 13. A. Ghatak, K. Thyagarajan, *Introduction to fiber optics* (Cambridge University Press, India, 2011)
- 14. O. Ziemann, J. Krauser, P.E. Zamzow, W. Daum, *POF handbook: optical short range transmission systems*, 2nd edn. (Springer publisher, German, 2008)
- 15. W. Daum, J.U. Krauser, P.E. Zamzow, Z. Olaf, *POF -polymer optical fibers for data communication* (Springer Publisher, New York, 2002)